

ORIGINAL CONTRIBUTION

Learning in a Competitive Network

WOLFGANG BANZHAF¹ AND HERMANN HAKEN

Universität Stuttgart

(Received 27 June 1989; revised and accepted 1 December 1989)

Abstract—We consider the abilities of a recently published neural network model to recognize and classify arbitrary patterns. We introduce a learning scheme based on Hebb's rule which allows the system's neuronal cells to specialize on different patterns during learning. The rule which was originally introduced by Kohonen is appropriately modified and applied to the competitive network under study. A variant of the learning dynamics is then derived from an energy functional characterizing the specialization state of the network. Simulations are presented to demonstrate the specialization process for different pattern distributions.

Keywords—Neural networks, Winner-take-all networks, Pattern recognition, Pattern classification, Self-organization, Unsupervised learning, Hebbian learning, Competitive learning, Specialization.

1. INTRODUCTION

The recent interest in natural and artificial neural networks has shed new light on an old question, the computational properties of systems which are composed of many subsystems. It was proposed by different authors (see, e.g., Amari & Arbib, 1982; Grossberg, 1982; Haken, 1979; Hopfield, 1982; Kohonen, 1977) that the collective phenomena showing up in such systems may be responsible for the astonishingly strong computational capabilities these systems demonstrate.

In this article we follow the philosophy Synergetics has developed over the last 20 years (Haken, 1973, 1983, 1987a, 1988a) applying the idea that any kind of pattern or structure may be described as a unique entity. Despite the fact that a pattern in general is built from a huge number of elements of a material substrate, we shall consider patterns as the modes of behavior of systems consisting of many subsystems. In 1987, one of us (Haken, 1987b, 1988b) introduced a model of grandmother cells organized in a competitive network. In this model, every cell is responsible for the recognition of a whole pattern. Before a recognition process is started, the prototype pat-

terns need to be loaded into the synaptic connections between the input units of the network and the grandmother cells.

In neural networks in general, the modes of behavior may be seen as interaction patterns between their elements—the neurons. Whereas in the inanimate world, interactions between elements are fixed by nature once and for ever; living beings have the capability to change these interactions, as it is demonstrated, for example, by the remarkable plasticity of synapses between real neurons. To study the adaptive properties of the aforementioned competitive network model we consider in this paper the network equipped with a local learning mechanism of Hebb-type (Hebb, 1949) which enables it to extract information from the environment while already working in the recognition mode. The learning rules applied here resemble in many aspects the rules studied by Kohonen (1982, 1987) and enable the network to learn in an unsupervised fashion.

An illustrative analogy from daily life—dunes of sand encountered at the beach—will serve to explain the main idea. Imagine a landscape of sandhills distributed stochastically on the beach. The wind provides an unspecific though fluctuating kinetic energy offer to the sandhills initially resting. The sandhills, originally constituting fluctuations, influence the air movement in such a way that a differentiation with respect to their use of kinetic energy sets in. Particular fluctuations cooperate, others compete with each other establishing over time the collective spatial modes which are called dunes. Due to limited resources, the occurring modes compete for kinetic

Acknowledgement: We wish to thank the Volkswagenwerk foundation for financial support.

Requests for reprints should be sent to Wolfgang Banzhaf, Mitsubishi Electric Corporation, Central Research Laboratory, 1-1, Tsukaguchi Honmachi 8-chome, Amagasaki, Hyogo, 661, Japan.

¹Now at Mitsubishi Electric Corporation, Central Research Laboratory, 1-1, Tsukaguchi Honmachi 8-chome, Amagasaki, Hyogo, 661, Japan.

energy leading finally to dominant and, on the other hand, extinct dune modes.

Turning back to neural networks, we must first recall that every grandmother cell in the network under study has connections to input cells which may be lumped together to form a vector \mathbf{A} called a synaptic filter, since the cells' action is just to perform a weighted sum of its inputs. If we now introduce a learning process according to these lines, i.e., a dynamics of the synaptic filters \mathbf{A} which results in changes of \mathbf{A} proportional to the cells' firing state, the original fluctuations get amplified. In order to be competitive, the learning process has to be constrained to a redistribution of synaptic efficacies in the filters \mathbf{A} . Rather than being generally allowed, an increase of synaptic strength at one site must be balanced by a decrease on the other sites of the same cell. A cell already firing above average for a certain pattern will learn to respond to it even better the next time that pattern is offered. A series of different patterns presented to the system will thus lead automatically to different synaptic filters of the adaptive grandmother cells. In other words, the environmental input generates a sort of pattern formation process in the filters of grandmother cells.

More specifically, let a number of different patterns M be presented to the system in an arbitrary order. Then the K cells of the network will specialize onto the different patterns and, depending on their frequency of occurrence, will learn to represent them on their synaptic filters.

This process of specialization constitutes the theme of the present paper and we shall propose in subsequent sections a particular learning scheme to implement the above ideas. We shall start with a slightly modified version of the Hebb-like learning rule Kohonen (1982) has studied and we shall end with a learning rule derived from an optimization principle imposed on the specialization state of the grandmother cells.

The further content is organized as follows: Section 2 formulates the learning scheme algorithmically, section 3 presents selected simulation results, and section 4 discusses the relations to some other learning schemes known from the literature.

2. THE NETWORK AND THE LEARNING ALGORITHM

In its simplest form, the network consists of 2 layers of units (cf. Figure 1): the input layer and the internal processing layer. Input units, the state of which is represented by a real-valued vector \mathbf{q}

$$q_i \in [-1, 1], \quad i = 1, \dots, N, \quad \sum_i q_i^2 = 1,$$

where q_i is the state of input unit i , communicate with the environment but have no internal commu-

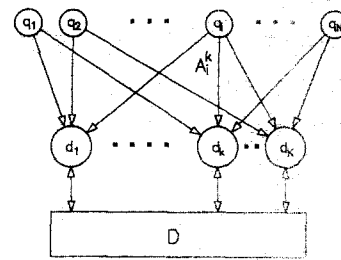


FIGURE 1. Design of the overall system. Information flow is coming in through input cells q , in layer I and is processed by layer II cells d_k . D means the global field $D = \sum_k d_k^2$.

nication. Internal layer units, on the other hand, are described by activities $d_k(t)$

$$d_k(t) \in [-1, 1], \quad k = 1, \dots, K$$

and get inputs from the former layer via synaptic connections A_{ki}

$$d_k^0 = \sum_{i=1}^{N_i} A_{ki} q_i, \quad (1)$$

as well as from the members of their own layer (via lateral connections).

The lateral connections are fixed and implement a dynamical competition between the K cells such that, after a transient time t_T , that cell k' has maximal absolute activity ($|d_{k'}| = 1$) which already started with the largest value $|d_{k'}^0|$. The winner takes all, that is, $d_k(t_T) = 0, \forall k \neq k'$, and the dynamics may be described by the following differential equation

$$\begin{aligned} \tau_f d_k &= d_k \left(1 - \sum_{k' \neq k} d_{k'}^2 - \sum_{k'} d_{k'}^2 \right) \\ &= d_k (1 - 2D + d_k^2). \end{aligned} \quad (2)$$

The lateral connections are inhibitory and of equal strength for all cells. Therefore, they may be substituted by a coupling of each cell to the global field D , defined as

$$D = \sum_{k'} d_{k'}^2.$$

The values d_k^0 serve as initial conditions for the competitive dynamics of the network. The dynamics itself was discussed in detail by Haken (1988b), and Haken and Fuchs (1988). Its ability to do face recognition was tested in a series of simulations reported in Fuchs and Haken (1988).

We now address the problem of how to learn adequate synaptic connections A_{ki} . The indications of the preceding section shall help us to implement a suitable learning algorithm. The synaptic connections should be able to vary over time

$$A_{ki} = A_{ki}(t),$$

and follow a dynamical learning rule we shall specify below.

At the beginning, the connections $A_{ki}(0)$ are distributed randomly. Thus, every cell starts out with an individual fluctuation for its synaptic filter \mathbf{A}_k , where the index k characterizes the k th grandmother cell, and has no predefined knowledge about the environment. The only condition we shall impose on the \mathbf{A}_k just from the very beginning is that the connections should be normalized:

$$\sum_i A_{ki}(t)A_{ki}(t) = \|\mathbf{A}_k(t)\|^2 = 1, \quad \forall k. \quad (3)$$

Although this condition seems to be rather artificial and we shall relax it later on, for the moment, we consider it necessary in order to arrive at a truly length-neutral similarity measure. For a fixed \mathbf{q} , this reads:

$$\begin{aligned} d_k^0 &= \sum_i A_{ki}(t)q_i = \mathbf{A}_k(t) \cdot \mathbf{q} = \|\mathbf{A}_k(t)\| \|\mathbf{q}\| \cos(\mathbf{A}_k(t), \mathbf{q}) \\ &= \cos(\mathbf{A}_k(t), \mathbf{q}) \quad \text{iff} \quad \|\mathbf{A}_k(t)\| = \|\mathbf{q}\| = 1, \quad \forall k. \end{aligned} \quad (4)$$

Presentation of an input pattern $\mathbf{1}$ will thus cause different activities of the K grandmother cells determined by \mathbf{A}_k which later on become amplified by the competitive dynamics between cells.

A natural choice for a learning rule is the following modified Hebb rule

$$A_{ki}(t+1) = \frac{A_{ki}(t) + a d_k(t+1) d_k^0 q_i}{\|A_{ki}(t) + a d_k(t+1) d_k^0 q_i\|}, \quad (5)$$

where the parameter a controls the learning velocity. A similar rule was already applied by Kohonen (1982) and Oja (1982) and it will serve us to establish a competition between cells for the presented patterns. One should keep in mind, however, that during the learning process (5), the competition between grandmother cells is going on. In this way a time dependence of the learning velocity is introduced. We distinguish both of these dynamics by requiring different time-scales, the competitive learning dynamics being five to ten times slower than the activity competition.

For definitiveness, let us write down both dynamical equations in a version discretized in time:

$$d_k(t+1) = d_k(t)(2 - 2D + d_k^2), \quad (6)$$

$$A_{ki}(t+\tau) = \frac{A_{ki}(t) + a d_k(t+\tau) d_k^0 q_i}{\|A_{ki}(t) + a d_k(t+\tau) d_k^0 q_i\|}. \quad (7)$$

The faster time-scale (6) is regarded as setting up the elementary time step, whereas the slower one is expressed as an updating of the corresponding evolution equation every τ th elementary time step. In eqn (7), the actual outcome of the competition between grandmother cells, $d_k(t+\tau)$, enters the dynamics.

An appropriate interpretation of this learning rule would read: *Every cell k learns a pattern (adapts to*

a pattern) \mathbf{q} to such a degree as it is able to fire during competition after the presentation of \mathbf{q} .

If we now recall that \mathbf{q} is one out of a whole set of training vectors

$$\mathbf{q} \in \{\mathbf{v}^{(1)}, \dots, \mathbf{v}^{(M)}\}$$

offered for discrete times T each, it becomes obvious that fluctuations initially present in synaptic connections \mathbf{A}_k experience amplification as a consequence of cells' firing in a series of presentations of training patterns. Through the training process, a third time-scale is introduced which is not allowed to be smaller than that of eqn (7), that is,

$$T > \tau.$$

The built-in tendency of the algorithm is that cells k try to fire with higher average activity as learning proceeds through the training steps. Stated in other words: Cells k tend to *specialize* on different patterns and to eventually divide the high-dimensional pattern space into portions the size of which is determined by their respective frequency of presentation.

Under the assumption of a stationary probability distribution of the environmental input vectors, a kind of stability should emerge in the sense that the total amount of redistributed synaptic strength reaches a minimum after enough training steps have been taken.

Another sort of stabilization is found in nature, the regulation of learning velocity a according to global quantities such as the age or maturation state of an organism (Wiesel & Hubel 1963). Furthermore, as Kohonen (1987) has pointed out, from an algorithmic point of view the learning process of a cell may also be stopped depending on its activity $d_k(t)$, i.e., $a = a(d_k)$. Various detailed models are reasonable, for example, dependence on maximum firing rate $d_{k,\max}$ or on average firing rate $\langle d_k \rangle$. The common effect in many of these models is a sharp falling off of the corresponding learning rate a when the specified quantity exceeds a certain threshold. Due to the self-stabilization of competitive learning in our model, we shall not use any kind of external stabilization.

As Oja (1982) has shown, learning rules of the above kind (5), (7), may be expanded under the condition $a \ll 1$. In our case, this yields (holding \mathbf{q}) the succeeding formula for the development of connections A_{ki} :

$$\begin{aligned} A_{ki}(t+\tau) &= A_{ki}(t) \\ &+ a d_k(t+\tau) d_k^0 [q_i - d_k^0 A_{ki}(t)] + O(a^2), \end{aligned} \quad (8)$$

where d_k^0 is the last measurement of starting overlap before competition has set in.

The normalization constraint for the filters \mathbf{A}_k now has been abandoned. As is shown in the Appendix, the dynamics (8) nevertheless tends to normalize the

filters, $\|\mathbf{A}_k(t)\|^2 \rightarrow 1$, during iterations. An appropriate starting state could be prepared by choosing random values

$$0 \leq A_{ki}(0) \leq 1, \quad A_{ki}(0) = O(1/N^2).$$

From (8) we can immediately derive a continuous equation (a has been absorbed into τ_s)

$$\tau_s \dot{A}_{ki} = m_k d_k^0 [q_i - d_k^0 A_{ki}], \quad (9)$$

where m_k may be either identical to d_k or equal to its time average over the fast dynamics of \dot{d}_k, τ_f

$$m_k = \langle d_k \rangle_{\tau_f}$$

A time-averaged quantity m_k cancels out all fluctuations below the time-scale τ_s . In order to generate a map, however, the relation between the two time-scales τ_s and τ_f should not exceed values of

$$\tau_s / \tau_f \leq 10.$$

Learning under such conditions we shall call nonequilibrium learning.

Here the question arises whether or not it would be possible to generate the learning dynamics (9) from a scalar potential function. It turns out that a slightly altered dynamical law

$$\tau_s \dot{A}_{ki} = m_k^2 d_k^0 [q_i (2 - \|\mathbf{A}_k\|^2) - A_{ki} d_k^0] \quad (10)$$

may be generated as a derivative of the following scalar functional

$$E(\mathbf{A}', \mathbf{q}) = - \sum_k m_k^2 d_k^0 \left[1 - \frac{1}{2} \|\mathbf{A}_k\|^2 \right] \quad (11)$$

as

$$\tau_s \dot{A}_{ki} = - \frac{\partial E}{\partial A_{ki}} \quad (12)$$

The Appendix shows that eqn (10) again tends to normalize filters. Rewriting the potential (11) as

$$E(\mathbf{A}', \mathbf{q}) = - \sum_{k=1}^K s_k^2 \times l_k^2 \quad (13)$$

where we introduced the following abbreviations:

$$s_k \equiv m_k(\mathbf{A}' \cdot \mathbf{q}) = m_k d_k^0,$$

and

$$l_k^2 \equiv 1 - \frac{1}{2} \|\mathbf{A}_k\|^2 \rightarrow \frac{1}{2} \text{ as } \|\mathbf{A}_k\|^2 \rightarrow 1,$$

we are led to the following interpretation: s_k measures the specialization of cell k on pattern \mathbf{q} . The greater d_k^0 at the beginning of competition between the K cells and the greater m_k reflecting the success of the competing cell k during competition, the greater s_k will be. $E(\mathbf{A}', \mathbf{q})$ measures the specialization of all cells.

Extending this result to the case where different patterns \mathbf{q} are given and the system is confronted

with them in an arbitrary order, we see that $\langle E \rangle_{\mathbf{q}}$ will be minimal if all the cells are specialized to a maximal degree. A global quantitative measure for the specialization of cells may be provided by the quantity

$$\left\langle \frac{1}{K} \sum_k s_k \right\rangle_{\mathbf{q}}$$

which can be termed the specialization parameter of the network.

In other words: The learning rule follows immediately from the requirement that it should optimize the ensemble average $\langle E \rangle_{\mathbf{q}}$ which measures the specialization state of the network.

The next section will deal with the simulation of different situations using the learning rules defined above.

3. SIMULATIONS

In order to demonstrate the feasibility of our approach, we present below simulation results for the learning rules eqns (7), (8), and (10). In general, the behavior of the rules was very similar, so we have chosen one example for each rule.

Simulation 1: $K > M$ —Generating redundancy

The first part of our simulation is devoted to the case where there are more grandmother cells ($K = 20$) than prototype patterns ($M = 6$). The aim is to show how the nonequilibrium learning rule (7) enables the system to generate redundant representations of patterns and stabilizes itself if the probability distribution of input is held constant.

We have chosen six one-dimensional analog patterns

$$v_i^m = \frac{\sin(i \cdot m^{1/0.7} \cdot \pi/10)}{\sum_i [\sin(i \cdot m^{1/0.7} \cdot \pi/10)]^2} \quad i = 1, \dots, 64, \quad m = 1, \dots, 6 \quad (14)$$

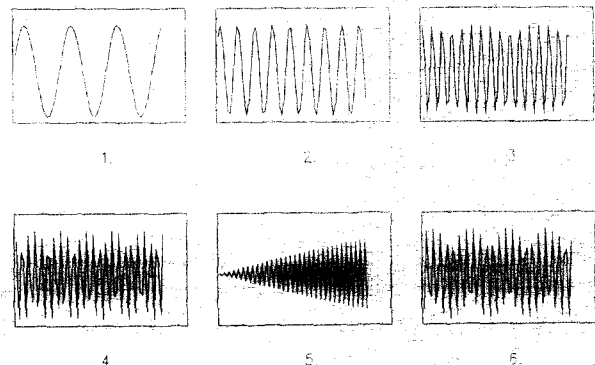


FIGURE 2. The six one-dimensional prototype patterns of simulation 1.

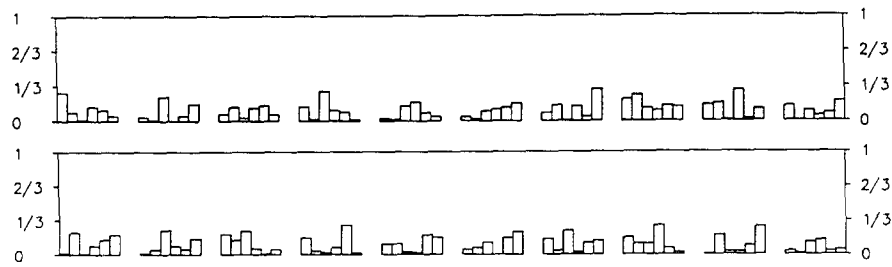


FIGURE 3. Activities $d_k^0 = A_k \cdot v^{(m)}$ at the beginning. First row: Histograms for cells $k = 1, \dots, 10$ reporting the different answers to the prototype patterns $m = 1, \dots, 6$. Second row: Histograms for cells $k = 11, \dots, 20$. Shown are the absolute values.

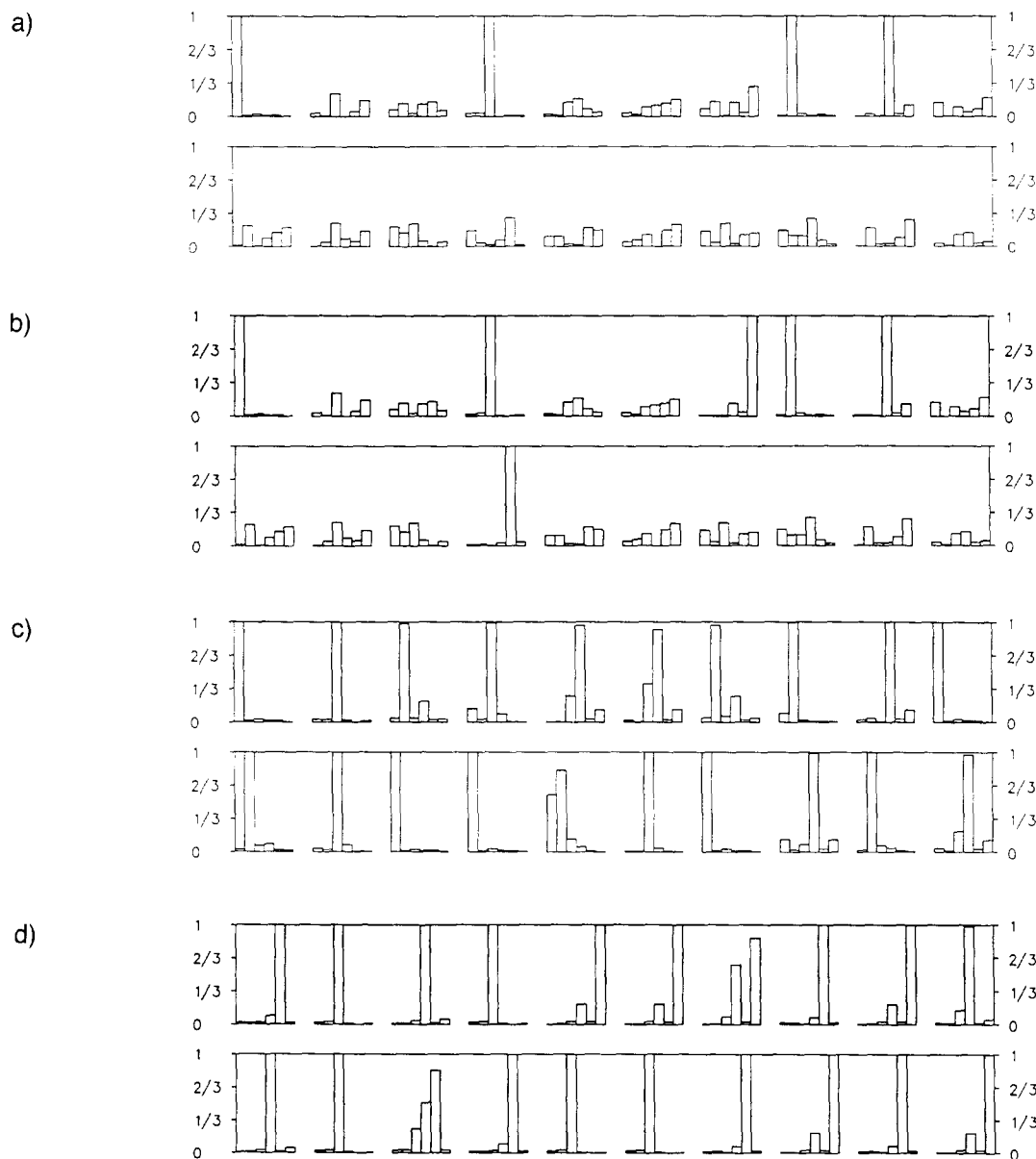


FIGURE 4. (a) *Equilibrium learning.* Activities $d_k^0 = A_k \cdot v^{(m)}$ after $r = 300$ training steps, phase I. First row: Same as Figure 3, second row: Same as Figure 3. Cells 1,8,4,9 have specialized on patterns 1,2,3,4, respectively. (b) *Equilibrium learning.* Activities $d_k^0 = A_k \cdot v^{(m)}$ after $r = 600$ training steps, Phase II. Cells 1,8,4,9,14,7 have specialized on patterns 1,2,3,4,5,6, respectively. All patterns are represented. (c) *Nonequilibrium learning.* Activities $d_k^0 = A_k \cdot v^{(m)}$ after $r = 1,000$ training steps, Phase I. All cells have specialized on patterns 1,2,3,4. (d) *Nonequilibrium learning.* Activities $d_k^0 = A_k \cdot v^{(m)}$ after $r = 4,000$ training steps, Phase II. All cells have specialized on patterns 3,4,5,6. Patterns 1,2 are completely forgotten.

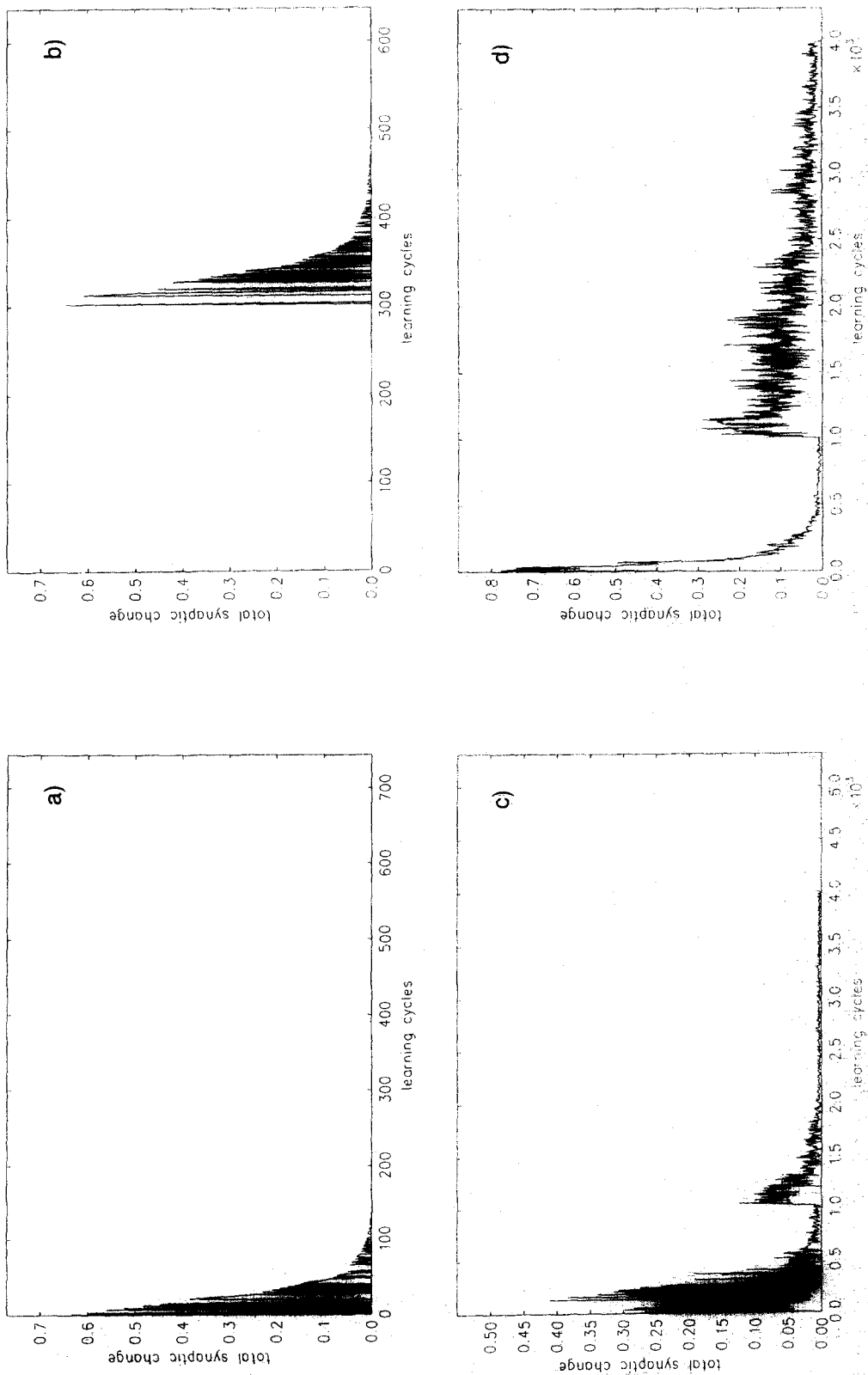


FIGURE 5. (a) Equilibrium learning. Total amount of synaptic redistribution according to (15) of cell 1 during Phase I and Phase II. (b) Equilibrium learning. Total amount of synaptic redistribution of cell 7 during Phase I and Phase II. (c) Nonequilibrium learning. Total amount of synaptic redistribution of cell 2 during Phase I and Phase II. (d) Nonequilibrium learning. Total amount of synaptic redistribution of cell 1 during Phase I and Phase II.

TABLE 1
Comparison of Expected (ex) and Measured (me) Outcome of Learning Under Nonequilibrium Conditions ($\tau = 10t_c$) in Simulation 1. Out of 20 Grandmother Cells $n_i^{(ex)}$ and $n_i^{(me)}$ Have Learned to Represent the Corresponding Patterns in Their Connections During Phase I and Phase II, Respectively

Pattern	n_i^{ex}	n_i^{me}	n_i^{ex}	n_i^{me}
1	10	5	0	0
2	5	6	0	0
3	2.5	4	4	5
4	2.5	5	2	3
5	0	0	6	6
6	0	0	8	6

(cf. Figure 2) represented by the activity of $N = 64$ input cells $q_i \in [-1, +1]$. Synaptic connections between input layer and processing layer are initialized by random values A_{ki} . The resulting synaptic filters for the K grandmother cells are then, however, normalized according to eqn (3).

Figure 3 shows the histograms of absolute activity values $|d_k^0|$ of all cells $k = 1, \dots, 20$ to stimulations with the six patterns (14) without competition. The dynamical equations (6), (7), are used to update activities during competition as well as synapses during learning. The elementary time step $t_c = 1$ is set by eqn (6).

We now contrast two situations with respect to the time-scale of learning:

- (a) $\tau = 300t_c$: Equilibrium learning: Competing cells have settled down in their equilibrium state before synapses are updated.
- (b) $\tau = 10t_c$: Nonequilibrium learning: Competing cells are still undecided

concerning the winner when synapses are updated.

In order to study stability of connection strengths once they have been formed, we trained in both of these situations with two different probability distributions of presented patterns following each other:

Phase I: $P(\mathbf{v}^{(1)}, \dots, \mathbf{v}^{(6)}) = (0.5, 0.25, 0.125, 0.0, 0.0)$,
 Phase II: $P(\mathbf{v}^{(1)}, \dots, \mathbf{v}^{(6)}) = (0.0, 0.0, 0.2, 0.1, 0.3, 0.4)$.

Whereas in Phase I patterns 5 and 6 are absent, in Phase II immediately following patterns 1 and 2 are not trained.

Figures 4 a,b show the resulting synaptic connections for equilibrium learning after 300 training steps (after Phase I) and after 600 training steps (after Phase II). Only one cell has become sensitive to an offered pattern regardless of its frequency of presentation. The change in probability distribution had no consequences for cells already specialized to patterns 1 and 2. Although synaptic plasticity was not turned off, the corresponding cells remained specialized on patterns which were not trained from steps 300 through 600. This stabilization is a consequence of the slow time-scale on which equilibrium learning occurs, leading first to a relaxation of cells' competition.

Figures 5 a,b confirm this picture by demonstrating the total amount of redistributed synaptic strength

$$\sum_i |\Delta A_{ki}| = \sum_i (|A_{ki}(t + \tau) - A_{ki}(t)|) \quad (15)$$

in cells k during training.

By contrast, Figures 4 c,d show the synaptic con-

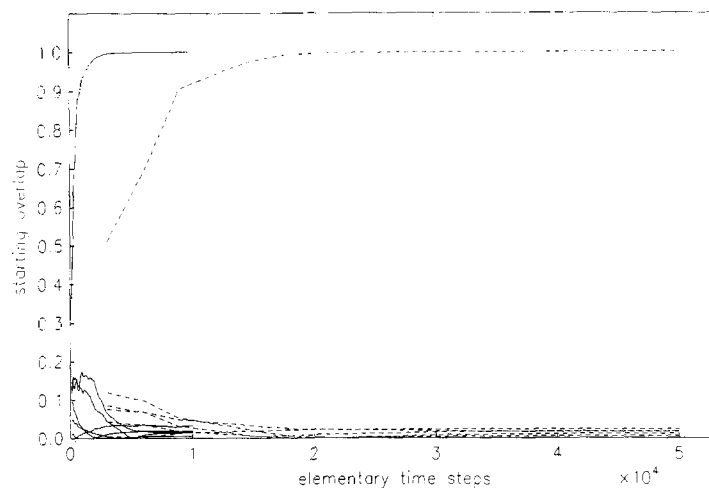


FIGURE 6. Development of starting overlaps for cell 1 over elementary time steps. Solid lines: Nonequilibrium learning. Broken lines: Equilibrium learning. Display was suppressed in the latter case for $t \leq 3,000t_c$.

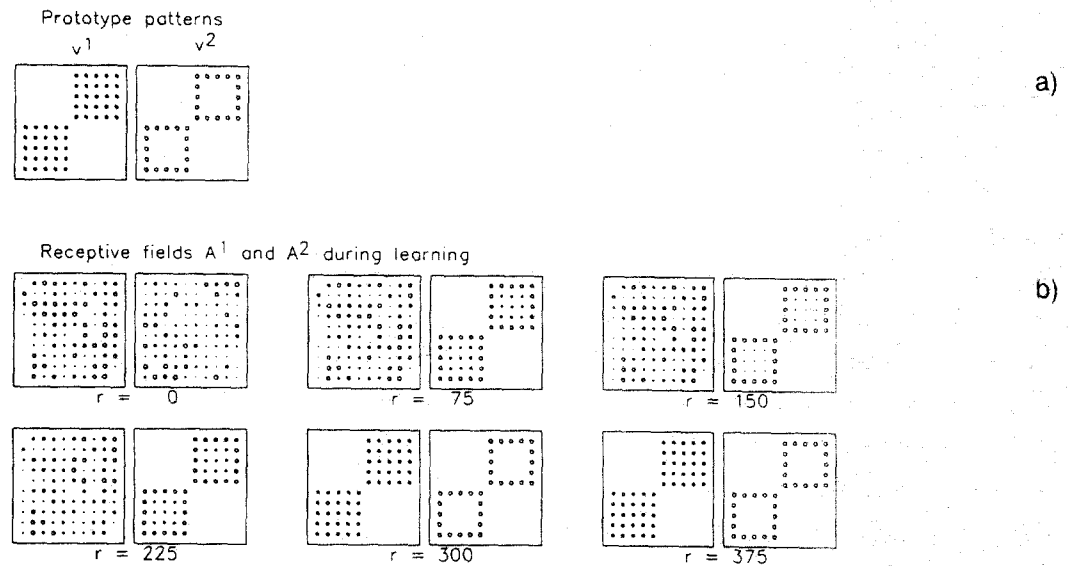


FIGURE 7. (a) Two geometrical prototype patterns. Activity of cells q_i is shown by magnitude of the corresponding circle. Activities are normalized. (b) Development of connection strengths A_1 and A_2 during learning. Between training step $r = 225$ and $r = 300$ cells have divided the pattern space into two portions.

nections after 1,000 training steps in Phase I and 4,000 training steps in Phase II under nonequilibrium learning conditions (recall the corresponding τ). Every cell has specialized to one of the offered patterns and a radical redistribution of synaptic strength occurred after the probability distribution of presented patterns was changed. Thus, the self-stabilization of learned patterns did not affect the ability of cells to further adapt as new events (patterns) occurred. This seems to be an important property of the nonequilibrium learning rule in this system since it is able to deal with unexpected situations.

Table 1 gives an overview of what has been expected by assuming a cells' specialization distribution

exactly following the probability distribution of presentations and what was the actual outcome of the learning experiment. A shift to unfrequent patterns is observed like in Kohonen's learning scheme (Kohonen, 1987). Figures 5 c,d show the total amount according to (15) for one cell keeping the same pattern and one cell changing its pattern during Phase II. Though to a certain degree stable, the adaptive properties are the dominant phenomenon here. As one can see, a redundancy is reached by nonequilibrium learning. No grandmother cell remains idle and, on the other hand, a possible destruction of a cell usually will not result in a complete disappearance of the corresponding pattern.

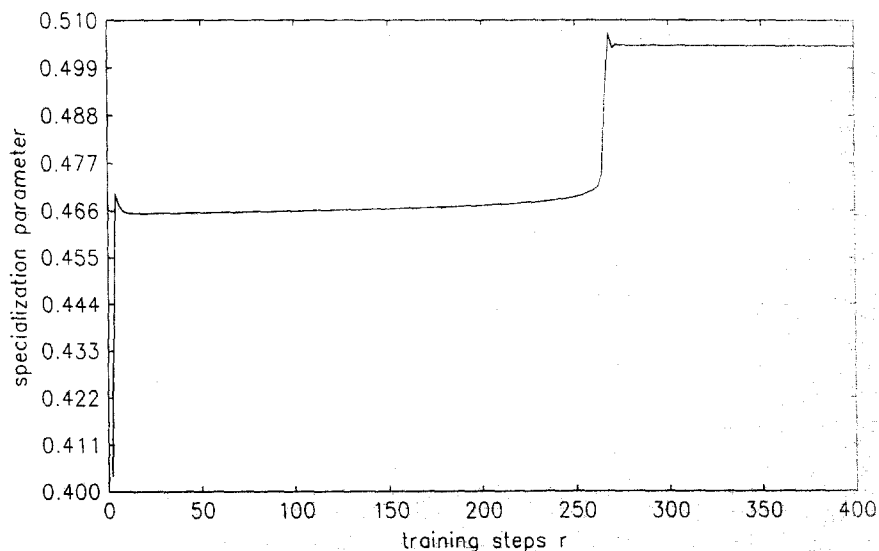


FIGURE 8. Behavior of the specialization parameter s (cf. eqn (16)) over learning steps.

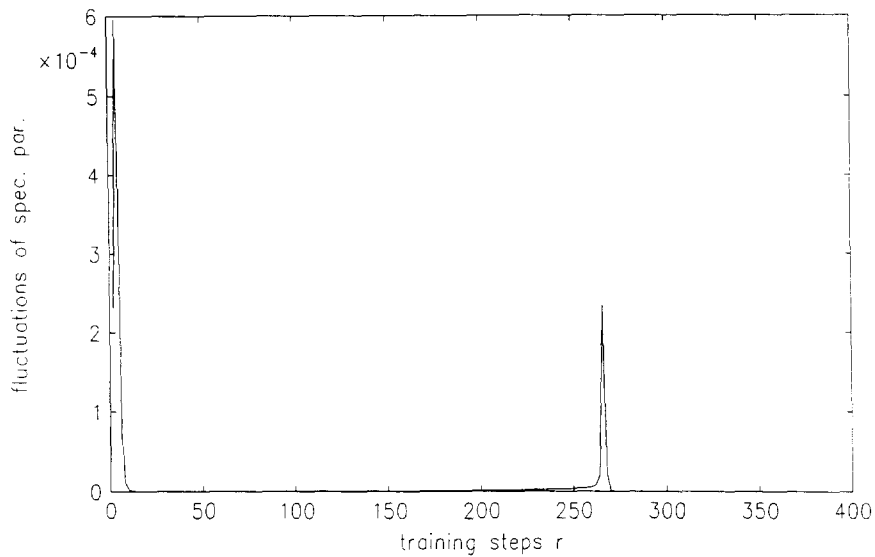


FIGURE 9. Fluctuations of the specialization parameter s , $\langle s - \langle s \rangle \rangle$ over learning steps. Besides the initial fluctuations a transition at $r = 266$ is indicated.

Figure 6 demonstrates how in both situations the starting overlap for all patterns approaches at a certain cell its stable values near 1 and 0. In elementary time steps, the nonequilibrium learning rule is much faster than equilibrium learning. For comparison purposes, we have to use the physical time as it is quantified in elementary time steps t_e rather than the number of training steps, since training steps differ greatly in the number of elementary time steps required for the equilibrium and nonequilibrium type of learning, respectively (see definitions above).

In conclusion, the nonequilibrium mode of learning has shown at least three advantages in being more adaptive, faster, and more effective, that is, more cells learn more patterns at the same time, than the equilibrium mode.

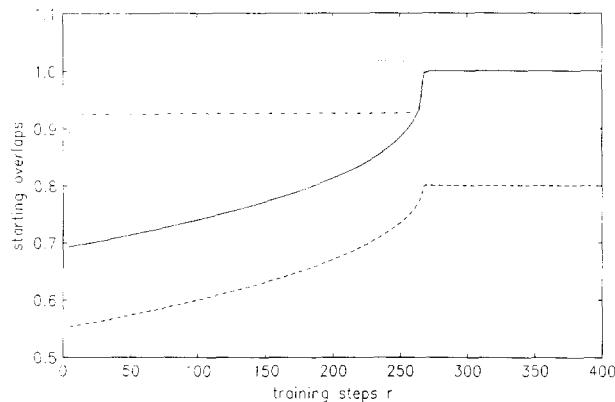


FIGURE 10. Starting overlaps d_k^q over training steps: Solid line: Cell 1, pattern 1; broken line: Cell 1, pattern 2; dotted line: Cell 2, pattern 1; broken/dotted line: Cell 2, pattern 2. At $r = 266$, the broken/dotted line becomes invisible, since it merges with the dotted line. Together, they quickly approach $d_k^q = 1$.

Simulation 2: $K = M$ —Observing a phase transition

The second simulation is concerned with the simplest case of an equal number of prototype patterns and grandmother cells, $M = K = 2$. The two-dimensional geometric patterns $\mathbf{v}^{(1)}$, $\mathbf{v}^{(2)}$ of Figure 7a are presented to a network of only two competing cells, the synapses of which are initialized by a random generator. Again, the patterns are normalized, but their *a priori* overlap is considerably high, $\mathbf{v}^{(1)} \cdot \mathbf{v}^{(2)} = 0.8$.

The patterns are trained in an alternating succession according to the second learning equation (8) and competition was allowed for 500 elementary time steps before changing the pattern. Nonequilibrium conditions for learning were realized by $\tau = 10t_e$.

Figure 7b shows the development of connections strengths \mathbf{A}_1 , \mathbf{A}_2 taken at different numbers of learning steps r . A fast adaptation of one cell to both of the (similar) patterns was accompanied by a nearly unchanged synaptic filter of the other. After 250 learning steps, however, length of the vectors representing the synaptic filters approached more and more the value 1 forcing the cells to decide on which of the patterns to specialize. A sharp phase transition is observed if the order parameter for specialization,

$$s = \left\langle \frac{1}{K} \sum_k m_k d_k^0 \right\rangle_q = \left\langle \frac{1}{K} \sum_k s_k \right\rangle_q \quad (16)$$

is measured (cf. Figure 8). The fluctuations of this parameter clearly show the transition in training step $r = 266$, see Figure 9. Figure 10 displays the evolution of the starting overlaps d_k^q for both cells and both patterns. Though cell 2 already was near to pattern 1, competitive learning forced it finally to

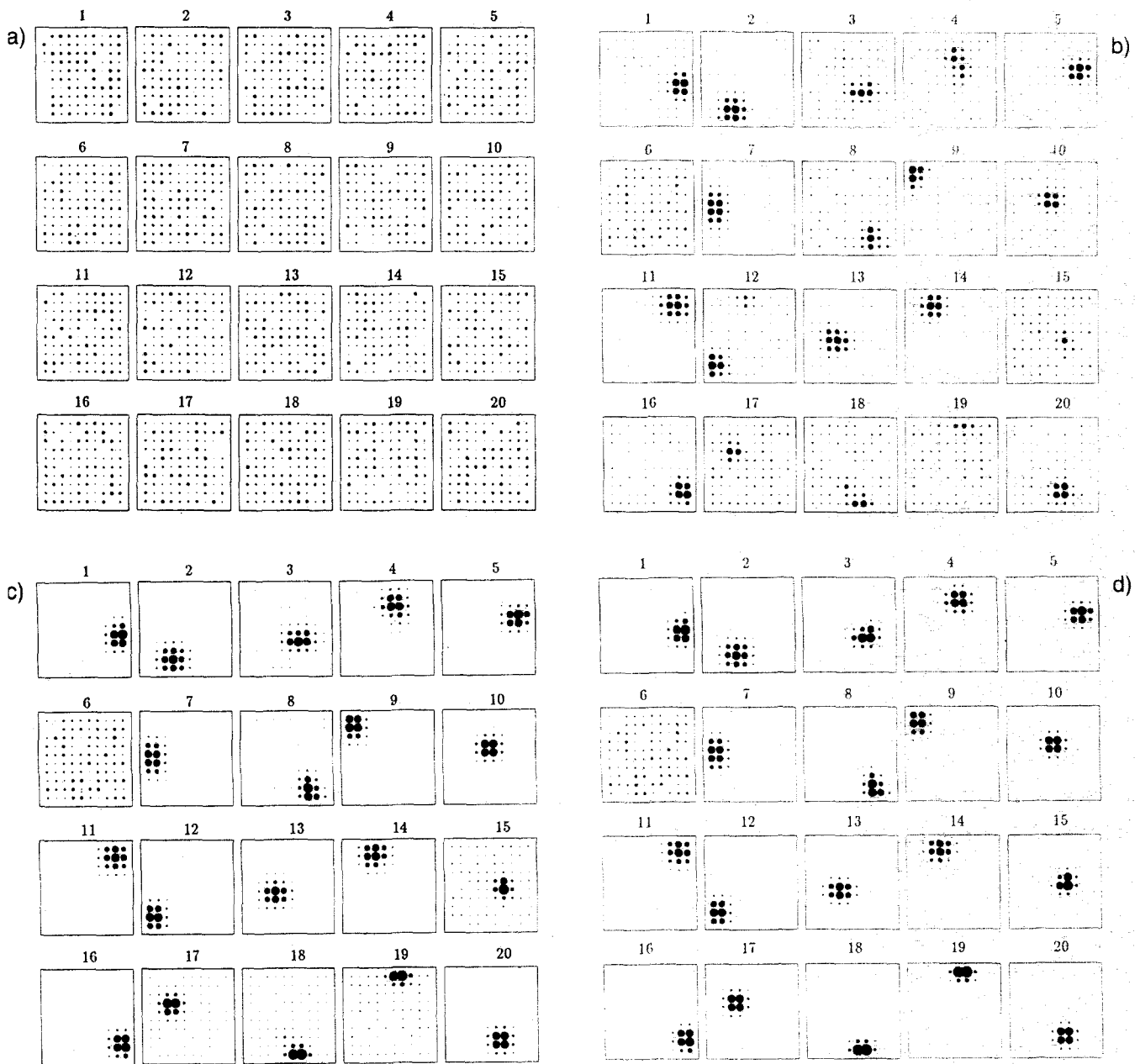


FIGURE 11. Development of synaptic connections of grandmother cells $k = 1, \dots, 20$ in Simulation 3: (a) Before learning: All cells cover the whole surface. (b) After $r = 1,000$ training steps. (c) After $r = 2,000$ training steps. (d) After $r = 4,000$ training steps. Synaptic strength proportional to the radius of black circles. Cell 6 was not able to adapt to any pattern.

specialize on the alternative pattern. Intermediate overlaps greater than 1 reflect the fact that learning was started without normalizing the connection filters.

The fact that both patterns were represented a long time on one cell may be interpreted as a tendency towards hierarchical clustering whereby high similarities between patterns are detected first.

Simulation 3: $K < M$ —Learning to classify

The last part of simulations deals with a typical classification situation where more patterns than recognizing cells are present. It will be shown that the

high-dimensional space of patterns will be divided by the learning dynamics into nearly equal portions.

The particular example we have chosen is an arrangement of sensory cells (input units) on a two-dimensional flat surface with $N = 100$ sensors q_{ij} . These are connected to a processing layer of $K = 2, 4, 8, 16, 20$ grandmother cells by initially randomized connections. No local constraint was implemented and the receptive field of every cell k therefore covers at the beginning the whole surface, see Figure 11a.

A training presentation is provided by a high stimulation q_{ij} at site i, j accompanied by a lower stimulation in its local neighborhood at sites $i' = i \pm l, j' = j \pm l, l = 1, 2, \dots$

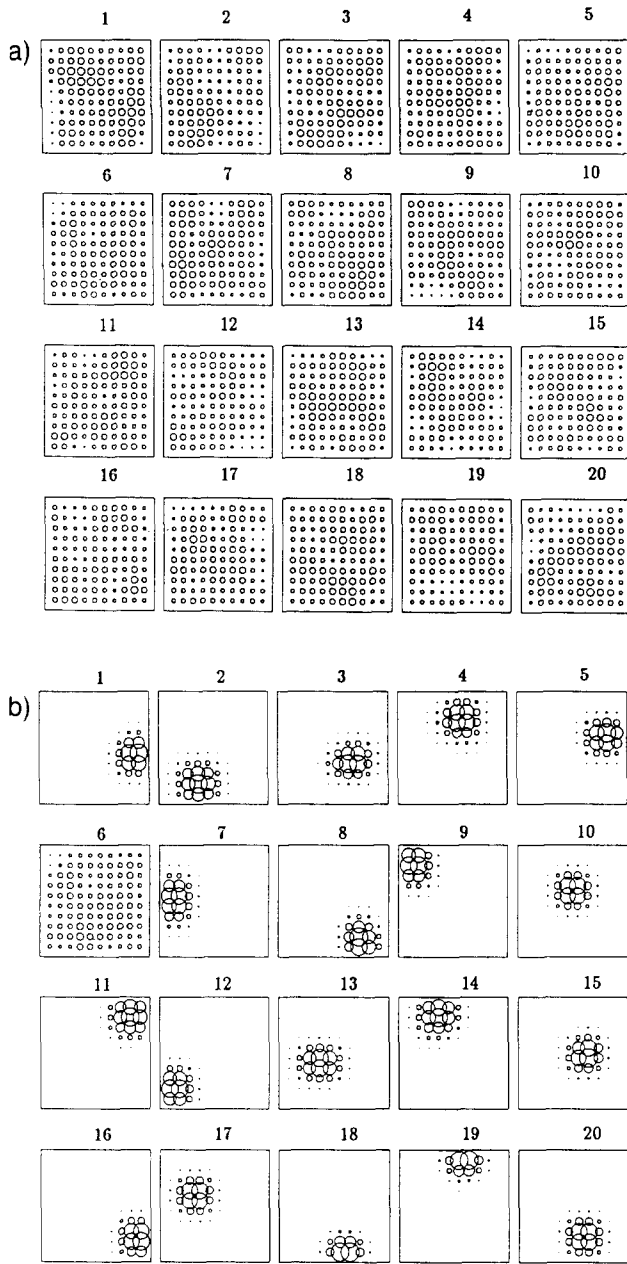


FIGURE 12. Starting overlaps d_k^0 , $k = 1, \dots, 20$ for the $M = 100$ patterns. (a) Before learning. (b) After $r = 4,000$ training steps. Activity to a pattern v^m indicated by radius of circles at position m, n .

The falling off is Gaussian in both dimensions. The idea here is that the system—if equipped with a diffusionlike interaction on sensory surface—is able to develop local receptive fields.

As is easily seen, the number of different patterns presented to the system is $M = 100$. The learning rule applied was eqn (10), discretized in time:

$$A_{ki}(t + \tau) = A_{ki}(t) + m_i^2(t + \tau)d_k^0[q_i(2 - \|A_k\|^2) - A_{ki}(t)d_k^0]. \quad (17)$$

Figures 11 b,c,d show the synaptic connections after $r = 1,000; 2,000; 4,000$ training steps, respectively. Here, the sequence of training patterns was

fixed once and repeated again and again. Though the energy decreased during learning, the global minimum (all cells specialized) was not reached due to the gradient learning strategy, eqn (12). One cell remained in its original state generated by random synaptic connections. This result should not astonish since there is no guarantee in the algorithm to converge to the global optimum.

After turning off competition, one can observe the reactions of cells to the $M = 100$ patterns (cf. Figure 12).

Figures 13 a–d show the results of runs with smaller numbers of grandmother cells. Training here was a random series of events at the sensory surface. Clearly, the cells have to cover more and more surface each and to classify inputs into broader and broader classes.

This simulation shows the following:

- (i) A diffusionlike interaction in sensory cells is sufficient in order to generate local receptive fields, if a suitable competition between cells is implemented. After maturation, learning and competition may be turned off.
- (ii) There is no built-in guarantee that the learning process will end up in the optimal solution, that is, maximal specialization of all cells. Rather, the general result will be a nearly optimal solution.
- (iii) The system is able to classify patterns and thus to learn from noisy input data. Though no pattern of the kind Figures 13 a–d was presented to the system, it nevertheless was able to develop a reasonable solution. As our unpublished results show, this carries over to other patterns. The system reaches a stable state characterized by small fluctuations in the redistributed synaptic strength.

4. DISCUSSION

The reader may have noticed many similarities of the presented learning scheme with Kohonen's learning algorithm and the formation of feature maps therein (Kohonen, 1987). As ours, Kohonen's learning could be termed nonequilibrium learning since it deals with an unrelaxed system at least if it is formulated dynamically. The adaption of Kohonen's feature maps to the probability distribution of the input vectors is known for many years (Kohonen, 1982). Hints on bound effects and on a shift in representation space towards regions with smaller probability density are also present in our system.

We see, however, the following major differences to Kohonen learning:

- (i) Our lateral interaction is uniform over the whole

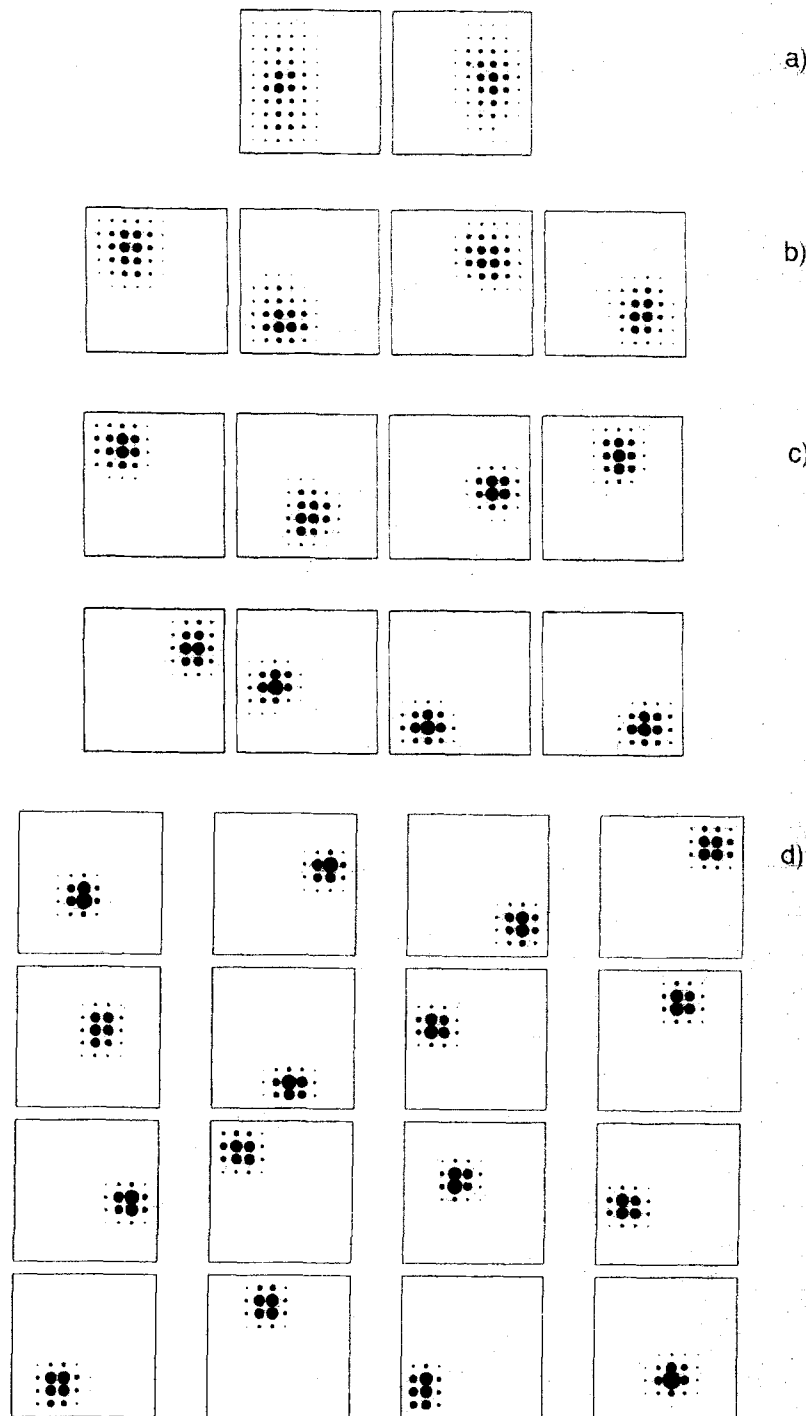


FIGURE 13. Resulting connections in different runs with (a) $K = 2$, (b) $K = 4$, (c) $K = 8$, (d) $K = 16$, cells. The sensory surface is divided in nearly equal portions.

cell space and constant in time. The only metric we have used is the similarity measure of overlap between patterns. No neighborhood topology whatsoever was defined in order to get a low-dimensional patterns representation called "topological map." Our system, however, generates a "scattered map" of the inputs, since if we turn off competition after a suitably defined maturation state of cells is reached, similar patterns will activate the same cells to a different degree with no reference to their respective spatial distribution.

- (ii) Stabilization of the learned representations is in our case a secondary effect of the specialization of cells leading to faster decisions during competition. No schedule for the sharpening of neighborhood interactions has to be implemented in order to stabilize learning. Again, this contrasts to Kohonen's scheme.
- (iii) In the later stages of learning, that is, when specialization progress is considerable, a general acceleration of the process is observed which could be used by decreasing the competition time in later stages.

As in the multilayer system of Linsker (1986), we could differentiate between a learning and a maturation stage. After learning decreases (signaled by decreasing fluctuations in the total amount of redistributed synaptic strength) learning with velocity a and competition dynamics (2) may be turned off to allow a further layer of cells to develop connections. In this way, an effective information compression may be reached without destroying valuable parts of the input information. Like in Linsker's scheme, an energy function was proposed here to determine the learning dynamics by the trend to minimize or maximize a certain function during the ongoing process. In our case, however, the synaptic connections as well as the patterns are continuous quantities. Moreover, the system learns superpositions of patterns, not principal components in the statistical sense.

The major difference to the competitive learning schemes of Grossberg (1987), Carpenter and Grossberg (1987), and Rumelhart and Zipser (1986) may be seen in the self-stabilization of the process as well as in its nonequilibrium character. To study, however, the relations between the proposed and other competitive learning systems (see, too, Mahlsburg, 1973; Nass & Cooper, 1975; and Takeuchi & Amari, 1979) goes far beyond the scope of the present paper and is left, together with a possible inclusion of local interactions and the extension to a multilayer system, for future investigation.

REFERENCES

- Amari, S., & Arbib, M. A. (1982). *Competition and cooperation in neural networks*. Berlin: Springer-Verlag.
- Carpenter, G. A., & Grossberg, S. (1987). ART2: Self-organization of stable category recognition codes for analog input patterns. *Applied Optics*, **26**, 4919–4930.
- Fuchs, A., & Haken, H. (1988). Pattern recognition and associative memory as dynamical processes in a synergetic system, Part I and II. *Biological Cybernetics*, **60**, 17–22 and 107–109.
- Grossberg, S. (1982). *Studies of mind and brain*. Dordrecht: D. Reidel.
- Grossberg, S. (1987). *The adaptive brain, Vol. I and II*. Amsterdam: North Holland.
- Haken, H. (1973). Synergetics—Cooperative phenomena in multi-component systems. *Proceedings of the Elmau Symposium on Synergetics 1972*. Stuttgart: Teubner-Verlag.
- Haken, H. (1979). Pattern formation and pattern recognition—An attempt at a synthesis. In H. Haken (Ed.), *Pattern formation by dynamical systems and pattern recognition* (pp. 2–19). Berlin: Springer-Verlag.
- Haken, H. (1983). *Synergetics—An introduction* (3rd ed.). Berlin: Springer-Verlag.
- Haken, H. (1987a). *Advanced synergetics* (2nd corr. print). Berlin: Springer-Verlag.
- Haken, H. (1987b). Synergetic computers for pattern recognition and associative memory. In H. Haken (Ed.), *Computational systems, natural and artificial. Proceedings of the Elmau International Symposium on Synergetics 1987*. (pp. 2–22). Berlin: Springer-Verlag.
- Haken, H. (1988a). *Information and self-organization*. Berlin: Springer-Verlag.
- Haken, H. (1988b). Nonequilibrium phase transitions in pattern recognition and associative memory. *Zeitschrift für Physik*, **B 70**, 121–123.
- Haken, H., & Fuchs, A. (1988). Nonequilibrium phase transitions in pattern recognition and associative memory: Numerical results. *Zeitschrift für Physik*, **B 71**, 519–520.
- Hebb, D. O. (1949). *The organization of behavior*. New York: Wiley.
- Hopfield, J. J. (1982). Neural networks and physical systems with emergent collective computational capabilities. *Proceedings of the National Academy of Sciences (USA)*, **79**, 2554–2558.
- Kohonen, T. (1977). *Associative memory—A system theoretic approach*. Berlin: Springer-Verlag.
- Kohonen, T. (1982). Self-organized formation of topologically correct feature maps. *Biological Cybernetics*, **43**, 59–69.
- Kohonen, T. (1987). *Self-organization and associative memory* (2nd ed.). Berlin: Springer-Verlag.
- Linsker, R. (1986). From basic principles to neural architecture, Part I, II, III. *Proceedings of the National Academy of Sciences (USA)*, **83**, 7508–7512, 8390–8394, and 8779–8783.
- Mahlsburg, C.v.d. (1973). Self-organization of orientation sensitive cells in the striate cortex. *Kybernetik*, **14**, 85–100.
- Nass, M. M., & Cooper, L. N. (1975). A theory for the development of feature detecting cells in visual cortex. *Biological Cybernetics*, **19**, 1–18.
- Oja, E. (1982). A simplified neuron model as a principal component analyzer. *Journal Mathematical Biology*, **15**, 267–273.
- Rumelhart, D. E., & Zipser D. (1986). *Feature discovery by competitive learning*. In Rumelhart, D. E., & McClelland, J. L. (Eds.), *Parallel distributed processing* (Vol. 1). Cambridge: MIT Press.
- Takeuchi, T., & Amari, S. (1979). Formation of topographic maps and columnar microstructures in nerve fields. *Biological Cybernetics*, **35**, 63–72.
- Wiesel, T. N., & Hubel, D. H. (1963). Effects of visual deprivation on morphology and physiology of cells in the cat's LGN. *Journal of Neurophysiology*, **26**, 978–993.

APPENDIX

In this Appendix we want to show the normalizing features of dynamical laws (8) and (10).

Squaring expression (8) for $A_k(t + \tau)$ gives:

$$\begin{aligned} \|A_k(t + \tau)\|^2 &= \|A_k(t) + a d_k d_k^0 [\mathbf{q} - d_k^0 A_k(t)]\|^2 \\ &= \|A_k(t)\|^2 + 2 a d_k (d_k^0)^2 [1 - \|A_k(t)\|^2] + O(a^2) \end{aligned} \quad (1)$$

where we have used the approximation

$$A_k \cdot \mathbf{q} \approx d_k^0. \quad (2)$$

From eqn (1) we can see immediately, that the length of vector A_k will increase in time step $t + \tau$ if it is smaller than 1 in step t and vice versa. A similar result holds for the continuous version (eqn (10)).

For eqn (10) we proceed as follows: Multiplying (10) by A_k^i and summing over i gives on the left:

$$\tau_s \sum_i A_k^i \dot{A}_k^i = \frac{1}{2} \frac{d}{dt} (\|A_k^i\|^2) \quad (3)$$

and on the right:

$$2 m_k^2 d_k^0 [1 - \|A_k^i\|^2], \quad (4)$$

again with the approximation

$$A_k^i(t) \cdot \mathbf{q} \approx d_k^0. \quad (5)$$

The equilibrium state is $\|A_k^i\|^2 = 1$, O.E.D.